Stochastic heterogeneity mapping around a Mediterranean salt lens

G. G. Buffett[1], C. A. Hurich[2] , E. A. Vsemirnova[3] , R. W. Hobbs[3] , V. Sallarès[4] , R. Carbonell[1] , D. Klaeschen[5] , B. Biescas[4]

[1]{ Institut de Ciències de la Terra "Jaume Almera", C. Lluís Solé i Sabarís s/n.

08028 Barcelona, Spain }

[2]{ Department of Earth Sciences, Memorial University of Newfoundland, Prince Phillip

Drive, St. John's, Newfoundland, A1B 3X5, Canada}

[3]{ Department of Earth Sciences, Durham University, Durham, DH1 3LE,

United Kingdom }

[4]{ Unitat de Tecnología Marina - Centre Mediterrani D'Investigacions Marines i

Ambientals, Psg. Marítim de la Barceloneta, 37-49 08003 Barcelona, Spain}

[5]{ Leibniz-Institute of Marine Sciences, IFM-GEOMAR, Duesternbrooker Weg 20,

D-24105 Kiel, Germany }

Correspondence to: G. G. Buffett (gbuffett@ictja.csic.es)

Abstract

We present the first application of stochastic heterogeneity mapping based on the band-limited von Kármán function to a seismic reflection stack of a Mediterranean water eddy (meddy), a large salt lens of Mediterranean water. This process extracts two stochastic parameters directly from the reflectivity field of the seismic data: the Hurst number, which ranges from 0 to 1, and the correlation length (scale length). Lower Hurst numbers represent a richer range of scale lengths and correspond to a broader range of reflection events. The Hurst number estimate for the top of the meddy (0.39) compares well with recent theoretical work, which required values between 0.25 and 0.5 to model internal wave surfaces in open ocean conditions based on simulating a Garrett-Munk spectrum (GM76) slope of -2. The scale

lengths obtained do not fit as well to seismic reflection events as those used in other studies to model internal waves. We suggest two explanations for this discrepancy: (1) due to the fact that the stochastic parameters are derived from the reflectivity field rather than the impedance field the estimated scale lengths may be underestimated, as has been reported; and (2) because the meddy seismic image is a two-dimensional slice of a complex and dynamic three-dimensional object, the derived scale lengths are biased to the direction of flow. Nonetheless, varying stochastic parameters, which correspond to different spectral slopes in the Garrett-Munk spectrum (horizontal wavenumber spectrum), can provide an estimate of different internal wave scales from seismic data alone.

1   Introduction

Mediterranean Water eddies, or "meddies", are large, warm, isolated lenses of highly saline Mediterranean Water that are found in the North Atlantic ocean. Mediterranean Water flows through the Strait of Gibraltar as an undercurrent [Bower et al., 2002], cascades down the continental shelf, while entraining less dense North Atlantic Central Water [Bower et al., 1997] and settles at depths between 500 and 1500 m [Richardson et al., 2000]. The undercurrent then rounds the corner of the Iberian peninsula at Cape St. Vincent, directed north by the Coriolis force. It is here that meddies form, spinning off the main undercurrent, translating westward and rotating anti-cyclonically [Serra et al., 2002]. Meddies were first reported in the western North Atlantic ocean by McDowell and Rossby [1978]. Since that time they have been found to be a common feature in the North Atlantic ocean [Richardson et al., 2000]). Many different aspects of meddies are currently being researched to understand their properties as well as their influence on large-scale mixing and climate [eg. Bashmachnikov et al., 2009].

Meddies have traditionally been studied using established oceanographic techniques, such as CTD (Conductivity-Temperature-Depth) probes to measure salinity and temperature [Ruddick, 1992] and acoustically tracked SOFAR floats [Armi et al., 1989]. Recently, seismic reflection profiling has been employed as a thermohaline imaging tool starting with the work of Holbrook et al. [2003] (eg. [Nandi et al., 2004; Nakamura et al., 2006; Buffett et al., 2009]). Holbrook and Fer [2005] used this technique to study internal waves in the Norwegian Sea. They found that horizontal wave number spectra derived from digitizing seismic reflector horizons in the open ocean compared favourably with the Garrett-Munk

spectrum [Garrett and Munk, 1975], which describes oceanic internal wave displacements. Biescas et al. [2008] performed the first detailed seismic analysis of a meddy. They found distinct seismic reflectivity differences in the upper and lower bounds of the meddy that are consistent with differences seen in historical temperature and salinity data. The upper boundary of the meddy was characterized by a few high-amplitude, laterally continuous reflections, whereas the lower boundary exhibited more numerous, shorter, lower amplitude reflectors.

To further understand meddy processes, we apply stochastic heterogeneity mapping to the study of a meddy in the Gulf of Cadiz (Figure 1). This method of statistically analyzing the reflection field of seismic data has been used extensively to study complex acoustic impedance variability in the solid earth (eg. [Goff et al., 1994; Holliger et al., 1994; Hurich and Kocurko, 2000; Carpentier and Roy-Chowdhury, 2007]) but, until now, has never been applied to the ocean.

Stochastic heterogeneity mapping is based on the premise that the seismic reflection wave field contains information on the spatial properties of the reflecting bodies and could thereby be used to extract quantitative information about the thermohaline finestructure of meddies. By extracting these parameters from a stacked seismic image of a meddy we can estimate the range of scales of its reflectivity patterns. In this way, we provide an estimate of the characteristic scales of internal waves of physical oceanographic processes directly from seismic data on zones of particular interest to oceanographers: the top and bottom [Biescas et al., 2008] and the sides of a meddy [Armi et al., 1989; Ruddick, 1992].

2   The Stochastic Model

The 1-D von Kármán model is described by three parameters: the correlation length (a), which is the upper limit for the scale invariance in heterogeneity [Carpentier, Ph.D. thesis, 2007], the Hurst number (ν), a measure of surface roughness or equivalently, the richness of the range of scales in the power law distribution (having values between 0 and 1), and statistical variance. We apply unit variance to standardize the distribution. For scale sizes smaller than the correlation length, the von Kármán model describes a power law (fractal) process, where ν represents its exponent. The parameter, ν relates to the fractal dimension (D) by

$$D = E + 1 - \nu, \qquad (1)$$

where E is the Euclidean dimension. For scales longer than the correlation length, the von Kármán model represents a process that is uncorrelated, such as white noise [Hurich and Kocurko, 2000]. The structure of the impedance field, and hence its autocorrelation, are in accordance with the defined power spectrum. This spectrum could take on a variety of forms. However, we choose a von Kármán stochastic distribution because it is capable of describing a band-limited power law process and has been thoroughly tested for this algorithm, albeit for deep crustal studies [Carpentier and Roy-Chowdhury, 2007]. However, the original work of Theodore von Kármán was to characterize random fluctuations in the velocity field of a turbulent medium [von Kármán, 1948], indicating that the method is also suited to the characterization of ocean fluid dynamics.

We express the analytic radial 2-D von Kármán power spectrum as [Carpentier, 2007],

$$P(k) = \frac{4\pi\nu a_x a_z}{(1 + k^2)^{\nu+1}}, \qquad (2)$$

where a_x and a_z are the correlation lengths in the lateral and vertical directions, respectively, ν is the Hurst exponent, k is the weighted radial wavenumber, $\sqrt{k_x^2 a_x^2 + k_z^2 a_z^2}$.

In the space domain, we express a 2-D autocorrelation function [Goff and Jordan, 1988],

$$C(r) = \frac{G_\nu(r)}{G_\nu(0)}, \qquad (3)$$

where $G_\nu(r) = r^\nu K_\nu(r)$, $K_\nu(r)$ is the second modified Bessel function of fractional order, and r the weighted radial autocorrelation lag, defined as $\sqrt{x^2/a_x^2 + z^2/a_z^2}$. $G_\nu(0)$ is defined according to Carpentier [2007],

$$G_\nu(0) = 2^{\nu-1}\Gamma(\nu), \qquad (4)$$

where the gamma function, $\Gamma(\nu)=(\nu-1)!$.

From here we shall refer to correlation lengths as scale lengths because, in band-limited fractal fields, these lengths give the threshold below which scaling is determined by a power law [Carpentier and Roy-Chowdhury, 2007] and due to the fact that the decorrelation length is the dominant visual scale of the fabric morphology. Furthermore, we restrict our

analysis to estimating horizontal scale lengths because determination of the vertical scale length is complicated by the estimation of source wavelet characteristics. This is because the source impulse is not a perfect spike, but is instead contaminated by side lobe energy, especially in the near offset traces [Yilmaz, 1987].

We estimate a_x and ν by performing a 2D Fast Fourier Transform, from which we derive a 2D power spectrum. We sum over the frequency direction and apply an inverse Fourier transform to obtain an autocorrelation function of NxM samples [Holliger et al., 1994; Carpentier and Roy-Chowdhury, 2007]. We choose window sizes to be representative of the areas of interest. Constraints are placed on window sizes to cover a minimum of 10 times the horizontal scale length, and at least 2 cycles vertically. Next, the 1-D analytic von Kármán autocorrelation function (Equation 4) is fitted to the calculated autocorrelation function using a model-space grid search and an L2 norm misfit, providing the estimate of a_x and ν. Temporal and spatial band-limiting of the broad-band von Kármán spectrum of the seismic data affects the accuracy of estimating ν, which can be overestimated by a factor of 2. Likewise, a_x can be underestimated by a factor of 3-6 [Carpentier and Roy-Chowdhury, 2007]. These errors are due to the fact that, although the impedance field is highly correlated to the reflectivity field, they are not equivalent. Nonetheless, they represent the current state of the art of stochastic heterogeneity mapping.

The stochastic heterogeneity mapping algorithm accounts for the fact that reflectors may have some apparent dip by performing dip searching so that the values are derived along the angle of maximum coherence. However, apparent dips are small: 3° on average across the seismic section, with a standard deviation of 0.3°.

3   Results

Under the premise that the statistical properties of the scattered wave field are highly correlated to the properties of the acoustic impedance field [Carpentier and Roy-Chowdhury, 2007], we analyzed a meddy in the seismic line GO-LR-05 acquired in the Gulf of Cadiz during the GO (Geophysical Oceanography) cruise of April and May, 2007 (Figure 1) for the distribution of the stochastic parameters Hurst number (Figure 2a) and correlation length (Figure 2b) around its margins. Four zones are described: The top of the meddy (A), the bottom of the meddy (B) and its sides (C and D). The stochastic parameters were extracted from the seismic section and overlaid using two different colour schemes. The mapping

5

procedure reveals the heterogeneity of the thermohaline-related fabric observed in the reflectivity field. Median and average Hurst numbers and scale lengths and their statistical distribution are reported in Figure 3.

Zone A exhibits middle to higher Hurst number values, with median and average values of 0.35 and 0.39, respectively. Zone B is dominated by lower Hurst numbers, having a median value of 0.14 and an average of 0.17. Zone C/D Hurst numbers both lie approximately between those of Zone A and Zone B, showing median/average values of 0.24/0.27 (C) and 0.23/0.26 (D). However, the distributions of Zones C/D Hurst numbers both resemble that of Zone A, in that there is an absence of the lowest values (those between 0 and 0.1). The majority of Hurst numbers for Zone A lie in the range between 0.15 and 0.5 (67%). In contrast, Zone B shows the dominant Hurst number distribution between 0 and 0.25 (80%). The majority of the Hurst numbers for Zones C and D fall between 0.1 and 0.5, 68% and 64%, respectively.

Scale lengths for Zone A are the highest of the four zones: 1120m (median) and 1310m (average). Zone B values are lower than those of Zone A, having median and average values of 946m and 1220m, respectively. Zones C/D show a predominance of lower scale lengths, with median/average values of 697m/961 m and 598m/980m, respectively. Further illustrating the difference between the sides and top/bottom: approximately 40% of scale lengths in Zones C and D are between 0 and 500 m, whereas only 12% and 22% of scale lengths for Zones A and B, respectively, lie in this range.

4   Discussion

The top of the meddy (Zone A), shows more lateral reflector continuity and a smaller variety of length scales than the bottom (Zone B). The Hurst numbers we obtained at Zone A (0.39) are in agreement with theoretical results Vsemirnova et al. [2009] modeled for open ocean conditions by emulating internal wave surfaces of a -2 slope Garrett-Munk spectrum (GM76). The Garrett-Munk spectrum describes the variation in internal wave energy in frequency and both vertical and horizontal wavenumber spaces [Garrett and Munk, 1975]. To simulate the GM76 slope they used Hurst numbers in a range of 0.25 – 0.50 with horizontal scale lengths of 5-10 km.

The scale lengths estimated from the seismic section are significantly lower than those used to model internal waves, even for Zone A (ca. 1 km compared to 5-10 km). This difference is possibly due to the factor of 3-6 underestimation that was reported by Carpentier and Roy-Chowdhury [2007]. Alternatively, the lower estimated scale lengths of the meddy may be explained by the fact that it is a dynamic, three-dimensional structure with currents that may be moving obliquely to the two-dimensional acquisition path. This is supported by an observation by Klaeschen et al. [2009], who estimated reflector motion by using an in-situ sound speed model near the NE edge of Zones A and B. They found longer horizontal wavelengths on the NE side of Zone A, as opposed to the SW side, and conclude that this is an indication of a different movement between the respective sides. Direct LADCP (Lowered Acoustic Doppler Current Profiler) measurements during the seismic acquisition confirmed that different parts of the meddy have different distributions of velocities, some along the path of the acquisition, some oblique to it [Klaeschen et al., 2009]. That is, the meddy was not simply in solid-body rotation, but was stretching slightly in a SW direction at the time of acquisition. This motion could disturb the reflector undulations that we observe, as measured by the extracted horizontal scale lengths. Since we are making a two-dimensional observation in a three-dimensional domain, the stochastic values we obtained are measurements of the component of the meddy motion in the plane of the seismic profile, rather than in the direction of meddy motion. Thus, we can expect our measurements of scale length to be shorter than theoretical predictions based on two-dimensional geometries.

Due to the band limiting of the seismic data, the scales observed are most likely confined to the lower extreme of meso-scale (2 − 200 km) size features. It follows that the stochastic parameters seen here are a reflection of the effects of internal waves, as seen in the Garrett-Munk spectrum, rather than smaller turbulent, ie. Batchelor scales [Batchelor, 1959]. The notably lower Hurst numbers seen at the bottom of the meddy (Zone B) may be partially a result of the fact that the frequency content of the source used in this survey (10-70 Hz) was too low to recover the smaller thermohaline staircases known to occur at the base of meddies [Ruddick 1992]. Thermohaline staircases are well-known structures in the ocean that range from tens to hundreds of meters thick and are found in regions where both temperature and salinity increase upward in a manner that promotes salt fingering processes [Schmitt 1994]. Given the low frequency source, we are only able to theoretically recover structures on the order of 5-75 m [Widess 1973]. Moreover, in practice, due to the thickness and sharpness of a reflecting interface, a safer upper estimate for maximum resolvable thickness would be

about double this estimate, between 10 and 150 m. It is plausible that the scales of some structures at the base of the studied meddy are smaller than those resolvable by this seismic source. Errors in Hurst number and scale length could be improved by inverting in-situ sound speed functions for acoustic impedance, thereby improving the certainty of correlation to the reflectivity field, upon which the stochastic parameters are extracted. Improving this certainty would also be useful to stochastic heterogeneity mapping studies of the solid earth where sufficiently sampled sound speed functions are practicably unachievable.

5 Conclusions

We partition our observation of Hurst number distributions for the meddy into three distinct zones: top, bottom and sides. Our calculations of Hurst number for the top of the meddy agree with recent theoretical work, which used values between 0.25 and 0.5 to model internal wave surfaces in open ocean conditions based on simulating a Garrett-Munk (GM76) slope spectrum of -2. The corresponding scale lengths (correlation lengths) mapped over the same reflectivity field, however, do not fit as well to specific seismic reflection events. We suggest two possible explanations for this discrepancy: (1) because the stochastic parameters are derived from the reflectivity field rather than the impedance field the estimated scale lengths may be underestimated; and (2) because the meddy seismic image is a two-dimensional slice of a complex and dynamic three-dimensional object, the estimated scale lengths are likely skewed to the direction of flow, where the theory is most applicable. Nevertheless, this work illustrates the potential of stochastic heterogeneity mapping as a seismic oceanography tool because it allows an estimate of lateral scale ranges of reflection events, and therefore actual physical oceanographic processes, such as internal waves. Finally, to improve upon errors in estimation of Hurst number and scale length in-situ sound speed functions could be inverted for acoustic impedance. In this manner stricter constraints on the degree of correlation to the reflectivity field, upon which the stochastic parameters are extracted could be obtained. These constraints, in turn, could be applied to solid earth studies, where such a sound speed function is practically unattainable.

References

Armi, L. D., D. Hebert, N. Oakey, J.F. Price, P.L. Richardson, H.T. Rossby, and B. Ruddick (1989), Two years in the life of a Mediterranean salt lens. J. Phys. Oceanog., 19:354–370

Bashmachnikov, I., F. Machín, A. Mendonça, and A. Martins (2009), In situ and remote sensing signature of meddies east of the mid-Atlantic ridge, J. Geophys. Res., 114, C05018, doi:10.1029/2008JC005032.

Batchelor, G. K. (1959), Small-scale variation of convected quantities like temperature in turbulent fluid. Part 1. General discussion and the case of small conductivity, J. Fluid Mech., 5, 113–133.

Biescas, B., V. Sallarès, J.L. Pelegrí, F. Machín, R. Carbonell, G.G. Buffett, J.J. Dañobeitia, and A. Calahorrano (2008), Imaging meddy finestructure using multichannel seismic reflection data. Geophys. Res. Lett., 35:L11609, doi:10.1029/2008GL033971, 2008.

Bower, A. S., L. Armi, I. Ambar (1997), Lagrangian Observations of Meddy Formation during A Mediterranean Undercurrent Seeding Experiment, J. Phys. Oceanog., 27, pp.2545-2575

Bower, A. S., N. Serra, and I. Ambar (2002), Structure of the Mediterranean Undercurrent and Mediterranean Water spreading around the southwestern Iberian Peninsula, J. Geophys. Res., 107(C10), 3161, doi:10.1029/2001JC001007, 2002.

Buffett, G.G., B. Biescas, J.L. Pelegrí, F. Machín, V. Sallarès, R. Carbonell, D. Klaeschen, R.W. Hobbs (2009), Seismic reflection along the path of the Mediterranean Undercurrent. Continental Shelf Research, doi:10.1016/j.csr.2009.05.017, 2009

Carpentier, S. (2007), On the estimation of stochastic parameters from deep seismic reflection data and its use in delineating lower crustal structure. PhD thesis, Universiteit Utrecht.

Carpentier, S., and K. Roy-Chowdhury (2007), Underestimation of scale lengths in stochastic fields and their seismic response: a quantification exercise. Geophys. J. Int., 169:547–562.

Garrett, C., and W. Munk (1975), Space-Time Scales of Internal Waves: A Progress Report, J. Geophys. Res., 80(3), 291–297.

Goff, J.A., K. Holliger, and A.R. Levander (1994), Modal fields: A new method for characterization of random seismic velocity heterogeneity. Geophys. Res. Lett, 21(6):493–496.

Goff, J.A. and T.H. Jordan (1988), Stochastic modeling of seafloor-morphology: Inversion of seabeam data for second order statistics. J. Geophys. Res., 93(6):13,589–13,608.

Holbrook, W.S. and I. Fer (2005), Ocean internal wave spectra inferred from seismic reflection transects. Geophys. Res. Lett., 32, L15604, doi:10.1029/2005GL023733, 2005.

Holbrook, W.S., P. Páramo, S. Pearse, and R.W. Schmitt (2003), Thermohaline fine structure in an oceanographic front from seismic reflection profiling. Science, 301:821–824.

Holliger, K., A.R. Levander, R. Carbonell, and R. Hobbs (1994), Some attributes of wave fields scattered from ivrea-type lower crust. Tectonophysics, 232:267–279.

Hurich, C.A. and A. Kocurko (2000), Statistical approaches to interpretation of seismic reflection data. Tectonophysics, 329:251–267.

Klaeschen, D., R.W. Hobbs, G. Krahmann, C. Papenberg, E. Vsemirnova (2009), Estimating movement of reflectors in the water column using Seismic Oceanography. Geophys. Res. Lett., 36, L00D03, doi:10.1029/2009GL038973, 2009.

McDowell, S.E. and H.T. Rossby (1978), Mediterranean Water: An Intense Mesoscale Eddy off the Bahamas. Science., 202. no. 4372, 1085 - 1087, DOI: 10.1126/science.202.4372.1085.

Nandi, P., W.S. Holbrook, P. Páramo, S. Pearse, and R.W. Schmitt (2004), Seismic reflection imaging of water mass boundaries in the Norwegian sea. Geophys. Res. Lett., 31, L23311, doi:10.1029/2004GL021325, 2004.

Nakamura, Y., Noguchi, T., Tsuji, T., Itoh, S., Niino, H., Matsuoka, T., 2006. Simultaneous seismic reflection and physical oceanographic observations of oceanic fine structure in the kuroshio extension front. Geophys. Res. Lett., 33, L23605. doi:doi:10.1029/2006GL027437.

Richardson, P.L., A.S. Bower, and W. Zenk (2000), A census of meddies tracked by floats. Progress in Oceanography, 45:209–250.

Ruddick, B. (1992), Intrusive mixing in a Mediterranean salt lens – intrusion slopes and dynamical mechanisms. J. Phys. Oceanog., 22:1274–1285.

Schmitt, R. W., (1994). Triangular and asymmetric salt fingers. J. Phys. Oceanog., 24(4): 855-860.

Serra, N., I. Ambar and R.H. Käse (2005), Observations and numerical modeling of the Mediterranean outflow splitting and eddy generation, Deep Sea Research Part II: 52, 383–408. DOI: 10.1016/j.dsr2.2004.05.025.

von Kármán, T. (1948), Progress in the statistical theory of turbulence. J. Mar. Res., 7:252–264.

Vsemirnova, E., R.W. Hobbs and A. Bargagli (2009), Testing recovery of ocean properties using an emulation of internal wave surfaces, Geophysical Research Abstracts, 11, EGU2009-1253, EGU General Assembly, Vienna.

Widess, M., 1973. How thin is a thin bed? Geophysics, 38:1176–1180.

Yilmaz, O., 1987. Seismic Data Processing, Soc. of Explor. Geophys.

Figures

Figure 1: Location of seismic profile and approximate trajectory of Mediterranean Outflow Water.
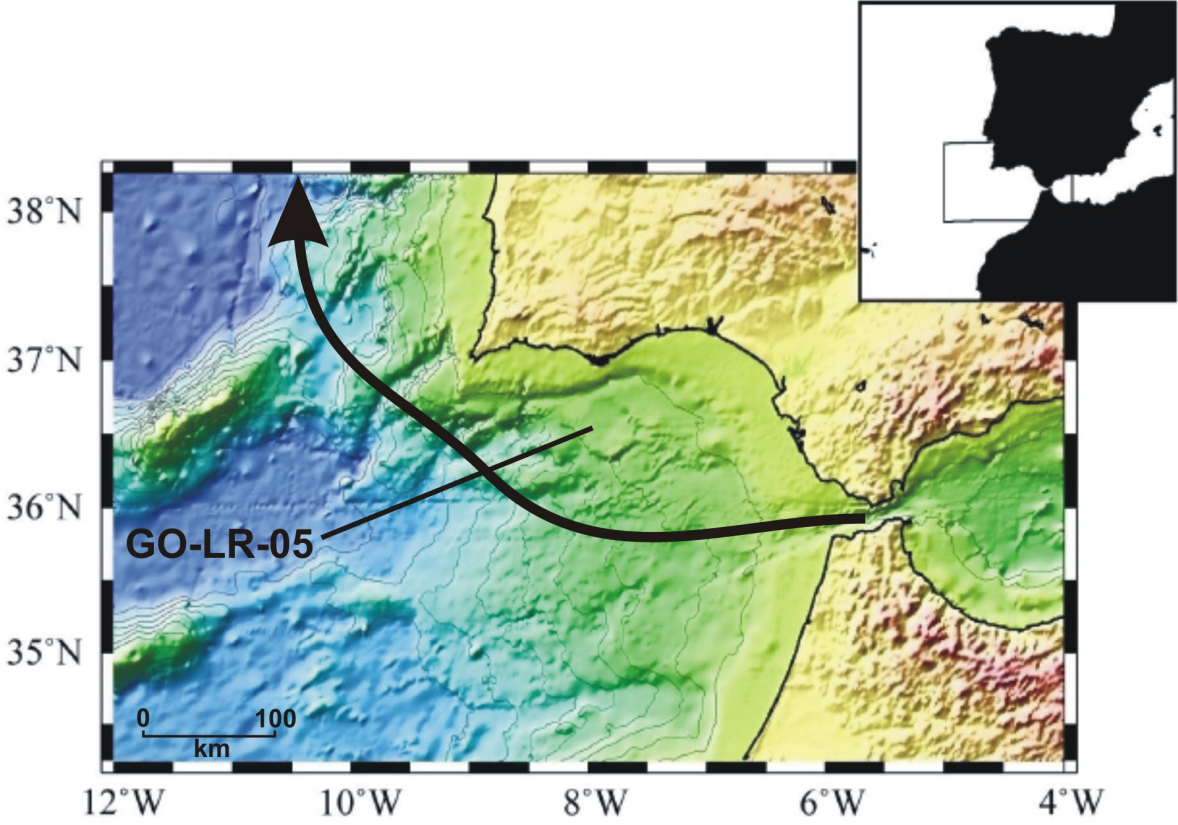
Figure 2: (a) Hurst number (ν), and (b) horizontal scale length (a$_x$) overlaid on seismic data along with stochastic parameter analysis boxes.
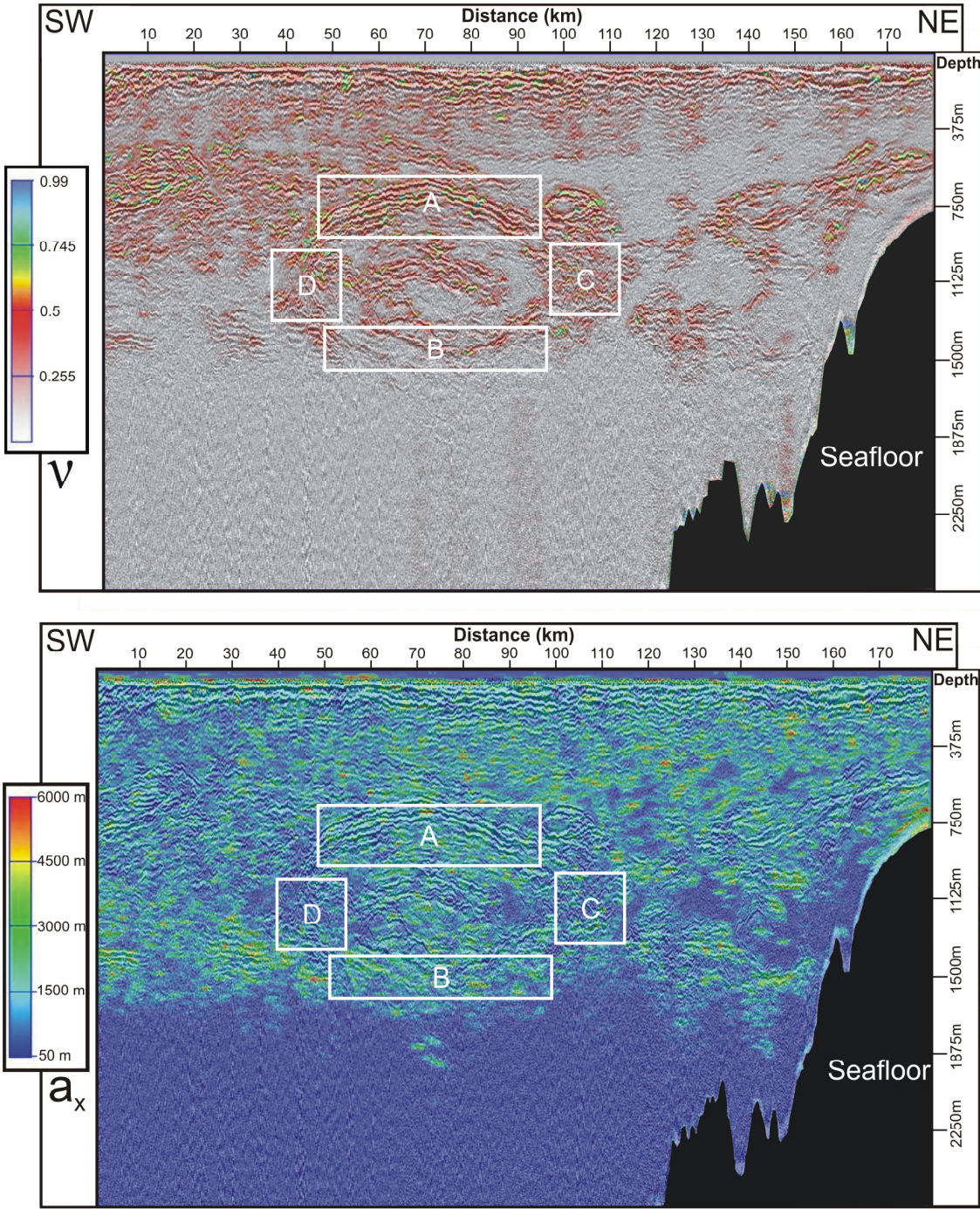
Figure 3: Histograms of analyzed meddy zones showing the statistical distribution of Hurst number (ν) and horizontal scale length (a_x). Left column: ν; Right column: a_x. Rows from top to bottom represent analyzed parts of the meddy, as outlined in analysis boxes (Figure 2). Values of ν were grouped into families incremented by 0.05 between 0 and 1. Values of a_x were grouped into families incremented by 500 m between 0 and 6500 m. Median and average ν and a_x were then calculated.